24

Dexterous Humanoid Whole-Body Manipulation by Pivoting

Eiichi Yoshida[1], Vincent Hugel[2], Pierre Blazevic[2], Kazuhito Yokoi[1] and Kensuke Harada[3]
[1]*AIST/ISRI-CNRS/STIC Joint French-Japanese Robotics Laboratory (JRL), (AIST),*
[2]*Laboratoire d'Ingenierie des Systemes de Versailles,*
[3] *Humanoid Research Group, Intelligent Systems Research Institute, (AIST)*
[1, 3]*Japan,* [2]*France*

1. Introduction

Recent progress in research on humanoid robots is making them to complicated tasks, such as manipulation, navigation in dynamic environments, or serving tasks. One of promising application areas for humanoid robots include the manipulation task thanks to their high potential ability of executing of a variety of tasks by fully exploiting their high mobility and adaptability coming from its large number of degrees of freedom. Especially, manipulating bulky objects through a whole-body motion is suitable for them, which has been difficult for other types of robots.

This paper focuses on whole-body manipulation of large objects by a humanoid robot using a method called "pivoting" (Y. Aiyama, et al, 1993). This manipulation method has several advantages such as dexterity and stability over other methods like pushing or lifting. Moreover, the requirement of maintaining the equilibrium of the robot during the manipulation cannot be managed in the same way as in the case of the robot simply walking. To cope with those problems, an impedance control framework is first introduced to hold and manipulate the object, together with a whole-body balancing control. Next, a control framework called resolved momentum control (RMC) (S. Kajita et al., 2003) is adopted to allow the robot to step forward after manipulation by keeping the hand position with the object.

The next section presents overview of the subject of manipulation tasks. Section 3 addresses an algorithm to deal with the manipulation, followed by the description of control techniques included in the algorithm in Section 4. Section 5 gives simulation results using the dynamic simulator OpenHRP. In Section 6 the simulated results of manipulation are verified by hardware experiments using HRP-2 humanoid platform described before concluding the paper.

2. Pivoting as dexterous manipulation method

For manipulation of large objects that cannot be lifted we can make use of "non-prehensile manipulation" methods such as pushing (M. Mason, 1986, K. Lynch, 2002) or tumbling (A.

Source: Humanoid Robots: Human-like Machines, Book edited by: Matthias Hackel
ISBN 978-3-902613-07-3, pp. 642, Itech, Vienna, Austria, June 2007

Bicchi, 2004). Aiyama et al. proposed a so-called "graspless manipulation" using pivoting motion (Y. Aiyama, et al, 1993), and also the analysis and planning have been reported by Maeda and Arai (Y. Maeda and T. Arai, 2003).
In another research field, whole-body manipulation tasks by humanoid robot have been investigated recently. The main manipulation methods developed so far are pushing (H. Yoshida et al., 2002, Y. Hwang et al., 2003, K. Harada et al., 2004, T. Takubo et al., 2004) and lifting (K. Harada et al, 2005).
We believe pivoting manipulation (Fig. 1), which we humans also often employ for example to move an oil drum or a barrel, is considered to be advantageous over those methods in for the following three reasons.

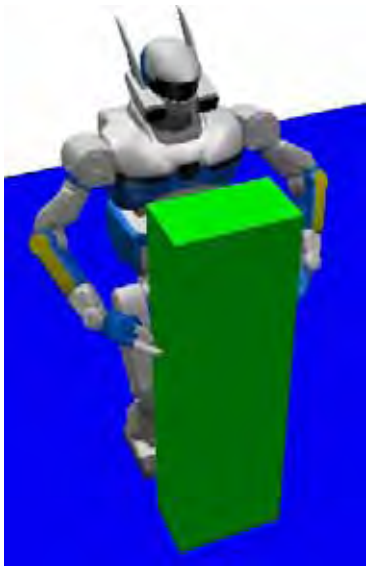

Figure 1. Pivoting manipulation by a whole-body motion of a humanoid robot

	Precise positioning	Adaptability	Stability
Pushing	×	×	○
Lifting	○	▲	×
Tumbling	▲	▲	○
Pivoting	○	○	○

○ : Suitable, ▲: Average, × : Not suitable

Table 1. Various manipulation methods compared for moving a large object by a humanoid

First, pivoting is expected to be precise in positioning. Since the object is not held in pushing, uncertainty is more significant than pivoting and tumbling has also limitation in reachability. Although some of those shortcomings can be overcome using sophisticated

control methods for pushing (K. Lynch, 1992, A. Bicchi, 2004) pivoting allows the robot to move the object to the desired position in a more straightforward manner.
The second advantage is the adaptability to various terrain conditions. Using pushing, it is difficult to be used in rough terrains whereas pivoting can be easily adapted. Lifting and tumbling can be used, but pivoting is more advantageous in terms of flexibility of manipulation and variety in shape and weight of manipulated objects.
Lastly, we can expect more stable manipulation through pivoting. It has advantage of lower risk of falling over lifting when manipulating large or heavy objects. Moreover, the manipulated object can help widening stability margin in some cases.
This comparison is summarized in Table 1. However, so far pivoting manipulation has not fully been exploited for humanoid robots due to the difficulty in coordinating manipulating motion with body balancing at whole-body level.
Therefore, the goal of this paper is to establish a control method for pivoting manipulation by a whole-body motion of humanoid robot. The contribution of this paper is two-fold: the algorithm for executing pivoting manipulation for a humanoid robot and integration of control techniques for this manipulation. For the first point, since pivoting manipulation that has not been implemented using humanoid platform so far, the challenge in this paper provides new potential application fields that need dexterous manipulation by humanoid robots. The second contribution addresses integration of such control techniques as impedance control for contact force, body balancing during manipulation and RMC for stepping motion for the purpose of whole-body manipulation. In the following sections, pivoting manipulation by a humanoid robot is presented based on those techniques.

3. Pivoting Manipulation Algorithm

The manipulation is executed by repeating the following two phases, the manipulation and robot motion phases.
In the former phase, the manipulation is done in a quasi-static way by repeating rotation of the object about an axis. The contact force to hold the object is controlled using impedance control. The manipulation is performed through whole-body motion coordination to achieve both manipulation and stable body balancing. The detailed descriptions are given in sections 4.1, 4.2 and 4.3.
In the latter phase, the robot itself moves to advance with the hands at the same position to continue manipulation. The body motion is planned through resolved momentum control (RMC) as detailed in section 4.4.
The algorithm of the pivoting manipulation task is summarized in Fig. 2. The detailed manipulation sequence is illustrated in Fig. 3 where the dotted and solid lines in each figure denote the states before and after the manipulation respectively.

a. The object is inclined by angle a around an axis a that includes a vertex v on the plane so that the object has a point contact with the plane at v (Fig. 3a).
b. The object is rotated by angle β around the vertical axis z on vertex v to move to the desired direction (Fig. 3b). As a result, the axis a *is* rotated to another axis $\boldsymbol{a}'$ on the plane.
c. The object is rotated by $-a$ around the rotated axis $\boldsymbol{a}'$ to reposition the front bottom edge of the object touches ground. The displacement of the object is defined as the distance between the projected points of its center of mass before and after the manipulation. (Fig. 3c).

1. If the displacement of the object exceeds a value D, the robot steps toward the desired direction.
2. Otherwise continue to step 1 or terminate the motion.

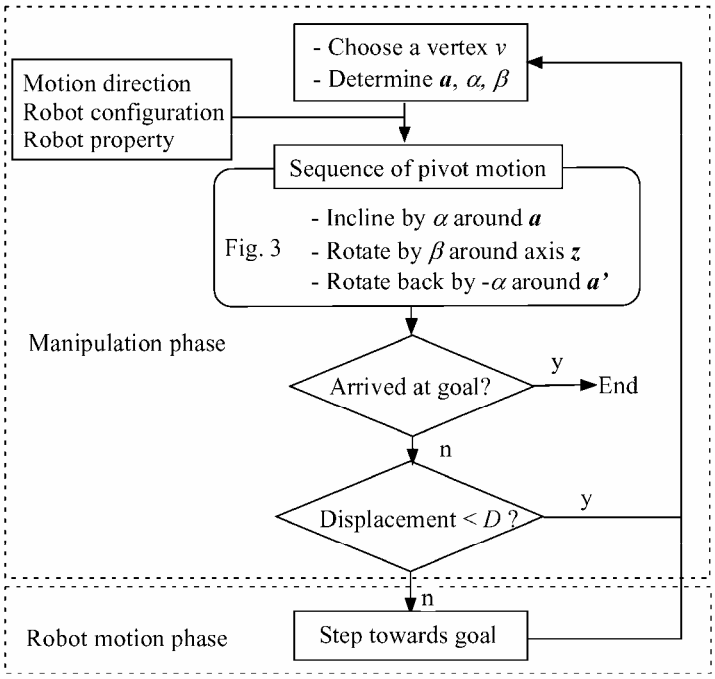

Figure 2. Flow of pivoting manipulation

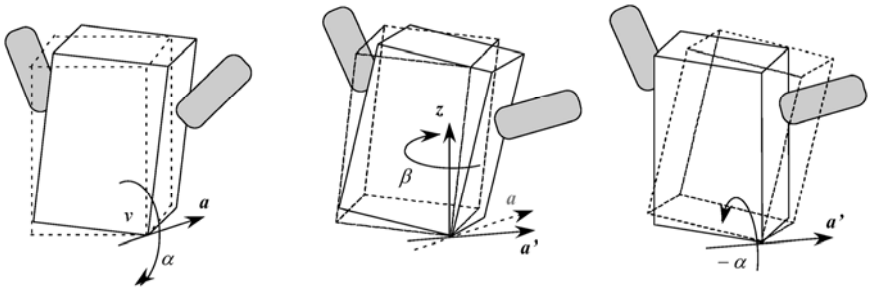

(a) Inclining (b) Rotating around z-axis (c) To initial contact

Figure 3. Sequence of pivot motion of a box object composed of three phases, (a) inclination, (b) horizontal rotation and (c) repositioning

According to the desired trajectory, the parameters a, β and D must be designed so that the manipulated object can follow the desired trajectory (Fig. 4). The working area and physical properties of the robot body must also be taken into account. The a axis and the vertex around which to incline the object are selected not to lose the stability of the robot and the object. In our case, the closer vertex to the robot is selected since smaller torque is required

for the movement, and the direction of axis *a is* chosen so that the robot does not make a large forward motion.
A vertical axis to the horizon is chosen as axis z since no work is required for quasi-static motion around this axis. The angle β depends on the constraint of robot motion capability as well as the desired trajectory of the robot. The hand trajectories can be calculated geometrically from the pivoting motion and contact points of the hand on the object. To execute more complicated trajectory than that of Fig. 4, we will further need a planning strategy to determine those parameters, taking account of combination of stepping motion. The next section details the manipulation control and robot motion for the pivoting task.

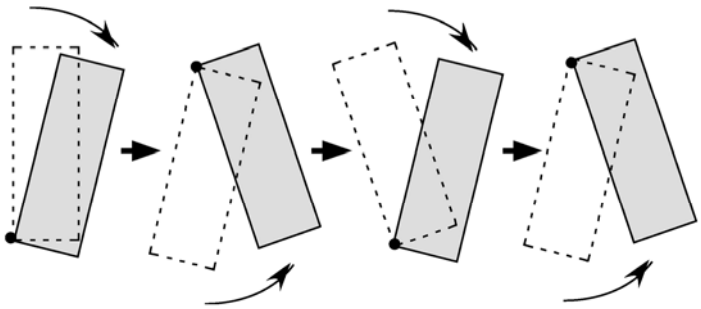

Figure 4. Sequence of pivoting manipulation to transport an object

4. Control Techniques for Manipulation and Robot Motion

In this section we describe how the manipulation task is controlled by a humanoid robot. In the manipulation control phase, the robot is supposed to grasp the object by two hands firmly (Fig. 1) without slipping. First, we introduce impedance control to control the contact force to hold the object. Then, a method of body balancing is adopted to maintain the center of mass (CoM) in the supporting phase during manipulation. We assume that the manipulation is done for a rectangular box-shaped object in a quasi-static way by repeating the rotations on a plane as described in Fig. 3.

4.1 Object holding

Since we assume quasi-static motion, we adopt position control for robot hands to achieve the trajectory for the desired motion. For position-controlled robot as HRP-2 used for simulations and experiments, the output of the following impedance control is added to the position command of manipulation to regulate the contact force (K. Harada et al, 2004). The robot hands are placed on the two sides of the object so that they can apply forces in the opposite directions. Let x_H be the hand position which is controlled in the direction perpendicular to the object face, and let f_x be the force exerted to the hand. The impedance control law to lead the force f_x to the desired force f_{xd} is given as

$$m\ddot{x}_H + c\dot{x}_H = f_{xd} - f_x \tag{1}$$

where m and c are the mass and damper parameters. This control scheme is illustrated in Fig. 5. For grasping, one of the hands is controlled by this law and the other is controlled in position to avoid unnecessary oscillation.

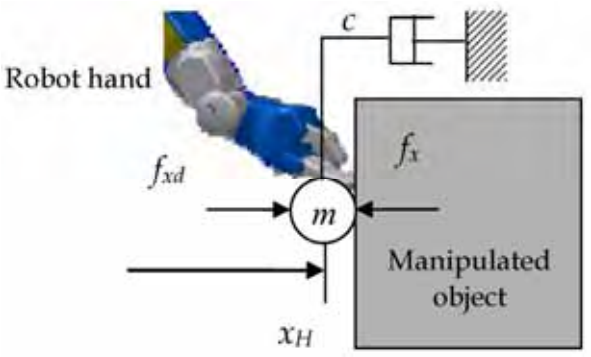

Figure 5. Impedance control for grasping based on force. To achieve the desired force f_{xd}, the output force f_x is computed by using impedance using virtual mass and damper parameters m and c

Since the humanoid robot HRP-2 we are using is based on position control, the control law is discretized in the simulation and experiment implementation as follows.

$$x_H(t + \Delta t) - x_H(t) = \frac{\Delta t^2}{m}\left(f_{xd} - f_x(t) - c\frac{x_H(t) - x_H(t - \Delta t)}{\Delta t} \right) + x_H(t) - x_H(t - \Delta t) \quad (2)$$

where Δt denotes the sampling period of robot control.

4.2 Pivoting Manipulation

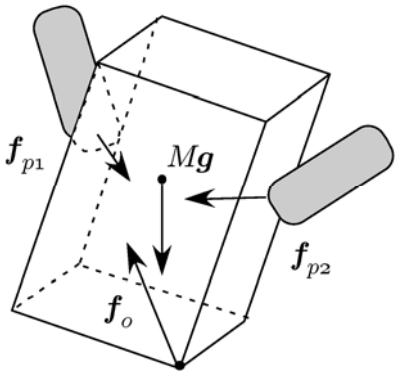

Figure 6. Forces for pivot motion using two contact points

We assume that the robot holds the object rigidly by two contact points of its hands as illustrated in Fig. 6. Let $\boldsymbol{p}_{pi}$, (i =1, 2) be the vector of position of each hand, p be the position of the center of gravity and $\boldsymbol{f}_{pi}$ be the force applied to each grasping point. Also, let Mg and $\boldsymbol{f}_0$ denote the gravity vector and resistance force at the contact point at the ground respectively. Then the object is in static equilibrium when the following conditions are satisfied.

$$f_o + \sum_{i=2}^{2} f_{pi} + Mg = o \tag{3}$$

$$\sum_{i=2}^{2} p_{pi} \times f_{pi} + p_g \times Mg = o \tag{4}$$

We assume that the manipulation is executed quasi-statically and that no slipping occurs at the contact points. We also assume that the geometry and location of the object are known. The object is manipulated by moving each hand under the above condition. The contact forces are controlled by impedance control (1) by giving the desired contact force f_{xd}.

4.3 Whole-body Balancing

The humanoid robot should not only apply the necessary force to the hand for manipulation but also keep the balance of the whole body throughout the manipulation task.

We adopt the method developed by Harada et al. (K. Harada et al, 2005). The key idea is to control the waist position in order that the "static balancing point" is on the center of the foot supporting polygon. The static balancing point $p_s=[x_s, y_s, 0]^T$ is the point on the floor to which all the resistance force from both hands and gravity are applied, which is equivalent to ZMP when only quasi-static motion is generated. The relationship between the contact force and static balancing point is described in the following equations.

$$x_s - \bar{x} = -\sum_{i=1}^{2} \frac{z_{pi} f_{pi}^x + (x_{pi} - x_s) f_{pi}^z}{M_R g} \tag{5}$$

$$y_s - \bar{y} = -\sum_{i=1}^{2} \frac{z_{pi} f_{pi}^y + (y_{pi} - y_s) f_{pi}^z}{M_R g} \tag{6}$$

where $f_{pi}= [\, f_{pi}^x, \quad f_{pi}^y \quad f_{pi}^z \,]^T (l = 1,2)$, $p_{pi}= [x_{pi}, y_{pi}, z_{pi}]^T$ and $g= [0,0,-g]^T$. The position of the CoM without external force is denoted by $\bar{p} = [\bar{x}, \bar{y}, \bar{z}]^T$ here and M_R is the total mass of the robot. Note that the sign in right-hand side of (5) and (6) is negative since the reaction force at each hand is $-f_{pi}$.

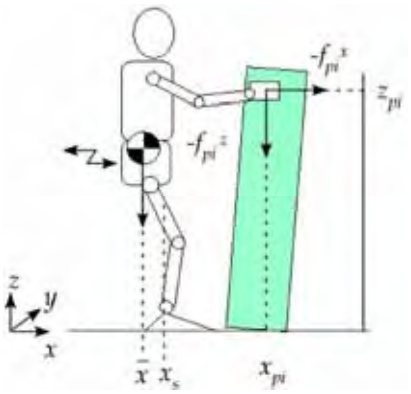

Figure 7. Body-balancing by moving waist position. According to the contact forces at the hands, the humanoid robot adjusts its waist position to maintain the "static balancing point" at the center of the support polygon

The balancing control is performed by moving the position of the waist so that the position of the static balancing point $\boldsymbol{p}_s$ is at a desired position inside the convex hull of supporting area(s) (Fig. 7). To ensure maximum stability margin, we usually employ the center of the support polygon as desired position of $\overline{\boldsymbol{p}}$. The movement of the waist position can be approximated by the CoM position !!!p from the desired position $\boldsymbol{p}_d$ of $\boldsymbol{p}_s$ (K. Harada et al, 2005).
In this way, the force of pivoting manipulation is generated as a resulting compensation of disturbance due to the contact with the object.

4.4 Stepping motion

Now the robot itself needs to move in the desired direction of object transportation after a sequence of manipulation that displaces the object to a more distant position from the robot. For this robot motion, it is preferable that robot keep the hands on the object to easily go on the manipulation.
We here introduce RMC that is a control framework where a humanoid robot is controlled such that the resulted total linear/angular momenta reach specified values (S. Kajita, 2003). It is well known that, for a humanoid robot to walk in a stable manner, the ZMP (Zero Moment Point) must be within the convex hull of the supporting area(s). By using RMC, we can control the CoM of the robot so that it is always within the convex hull of the supporting area(s) to maintain robot balance. Since the linear momentum $\boldsymbol{P}$ depends on the time derivative of CoM position $\boldsymbol{p}_g$ through the total mass M_R as $\boldsymbol{P} = M_R\dot{\boldsymbol{p}}_g$, the position of CoM can be controlled by manipulating the linear momentum as $\boldsymbol{P} = kM_R(\tilde{\boldsymbol{p}}_g - \boldsymbol{p}_g)$, where the tilde denotes the reference value, and k is the gain of the control scheme. Using this equation we are can calculate the desired linear momentum P to control the robot CoM.
The hand position can be controlled based on an extended method of RMC developed by Neo et al. (N. E. Sian, 2003) by keeping the position of CoM inside the supporting area. In this way, the robot can step towards the object with its both hands at the position keeping the contact, while the CoM is controlled always inside the convex hull of supporting area(s). Moreover, keeping the hand position on the object may help to maintain the equilibrium of the robot body.

5. Simulation results

To validate the proposed pivoting manipulation method, simulations using the humanoid robot HRP-2 (K. Kaneko et al., 2004) have been conducted using the humanoid robot simulator OpenHRP (F. Kanehiro et al., 2001). The humanoid robot HRP-2 has 30 degrees of freedom with 1.54 [m] in height and 58 [kg] in weight, with wrists and ankles equipped with force sensors. Since the input of force sensor is noisy, we use an average value of the last 20 samplings measured every 5 [ms]. The width, depth, and height of the object are 0.35[m], 0.2[m], and 1.2[m] respectively, with the mass of 3[kg].
In Table 2, the parameters of the pivoting sequence are shown. The directions of axes x, y and z are given in Fig. 8(a). Here parameter D of object displacement is set to 50[mm] to prevent the arms from going into singular stretched configuration and also from losing stability by extending arm too much. In the impedance control we adopt m = 10[kg], c = 300[N m^{-1} s] and f_{xd}= 25[N] respectively. The contact force f_{xd} is determined for the robot to hold firmly enough to prevent the object from slipping because of gravity. The z position of

contact point is set to 0.62[m] height and at the midpoint of the depth of the object in x direction.

In the simulation, first the robot grasps the object rigidly at the tip of the hands and keeps the hands at the original position until the contact force by impedance control stabilizes. The hand trajectories during the manipulation are computed geometrically by using the contact points of both hands and the motions described in Table 2. Position control is performed to follow the calculated hand trajectories and the impedance control law (1) is applied to one of the hands, in our case the right hand, to maintain grasping during the manipulation while as the other hand is position-controlled.

Fig. 8 shows the snapshots of the simulation. As can be seen, the humanoid robot successfully displaces the object by pivoting.

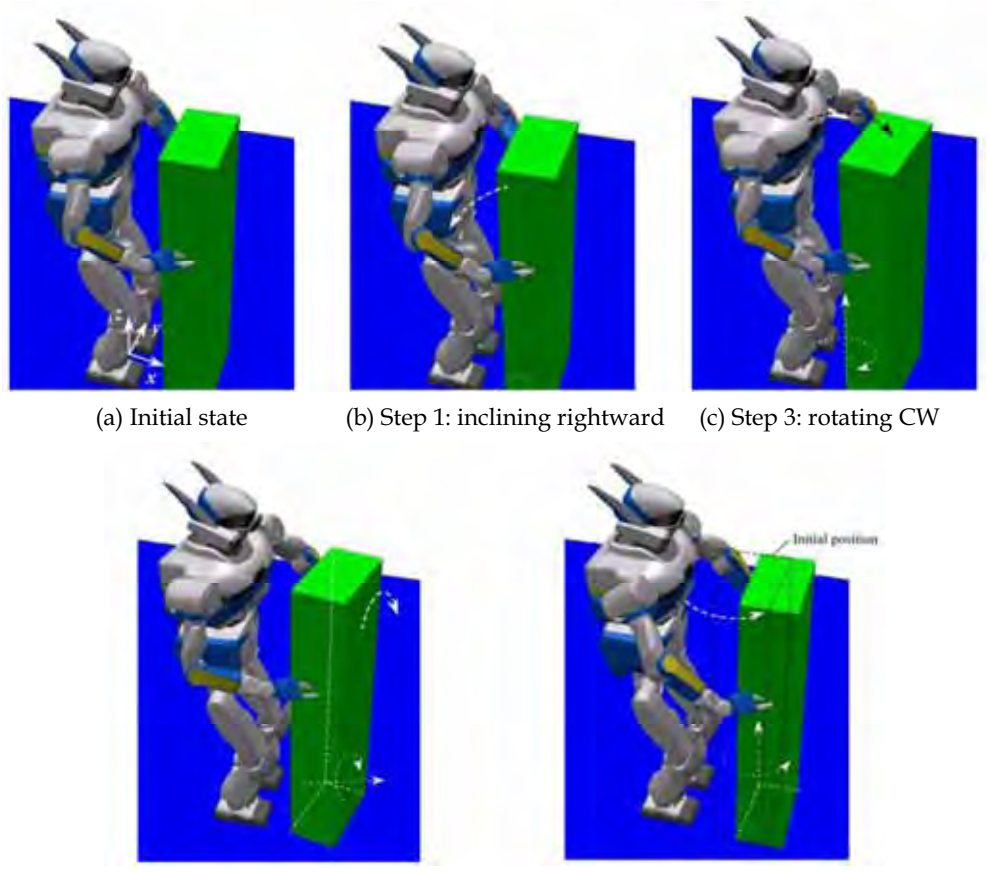

(a) Initial state (b) Step 1: inclining rightward (c) Step 3: rotating CW

(d) Step 4: inclining leftward (e) Step 5: rotating CCW

Figure 8. Simulation results of pivoting manipulation. Starting from the initial state (a), first the robot inclines the object (b) to support it on a vertex and then turns it horizontally clockwise (c). After repositioning in a horizontal position, the object is inclined on the support of another vertex (d) and turned counter-clockwise to advance the object in a parallel position with the initial one

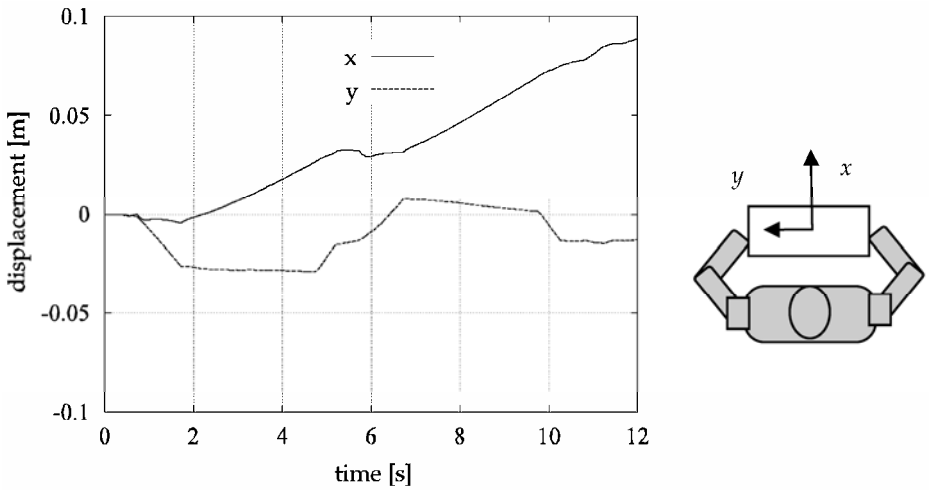

Figure 9. Simulation result of displacement of the center of mass of the manipulated object in x and y directions shown at right-hand side

Step	Type (in Fig. 3)	Axis*	Angle [deg]	Time [s]	Contact vertex **	Description**
1	(a)	$\boldsymbol{a}_1$= (3, -1, 0)	α = 5.0	1.0	NR	Inclining rightward
2	(b)	z= (0, 0, 1)	β =-15.0	3.0	NR	Rotating CW
3	(c)	$\boldsymbol{a}'_1$= (3, -1, 0)***	α = -5.0	1.0	NR	Inclining back
4	(a)	$\boldsymbol{a}_2$= (3, 1, 0)	α = -5.0	1.0	NL	Inclining leftward
5	(b)	z= (0, 0, 1)	β = 15.0	3.0	NL	Rotating CCW
6	(c)	$\boldsymbol{a}'_2$= (3, 1, 0)***	α = 5.0	1.0	NL	Inclining back

* See Fig. 8a for the reference frame. The angle between the axis $\boldsymbol{x}$ and $\boldsymbol{a}_1$, $\boldsymbol{a}_2$ is 18.4 [deg] and -18.4[deg] respectively.
** NR: Near-Right, NL: Near-Left, CW: Clockwise, CCW: Counter-clockwise
*** Axis $\boldsymbol{a}'$ is rotated vector a around z by β.

Table 2. Parameters of pivot motion

In the simulation, we measure the displacement of the manipulated object, the contact forces, and center of the mass of the robot respectively to evaluate the performance of the manipulation itself, impedance control, and the balance control.
The displacement of the center of mass of the manipulated object projected on the ground is shown in Fig. 9. Since the object is first inclined around the axis a before rotating around z

axis, the x displacement reduces first and then increases. This occurs twice and we can see the object is displaced by 0.073 [m] in x direction.

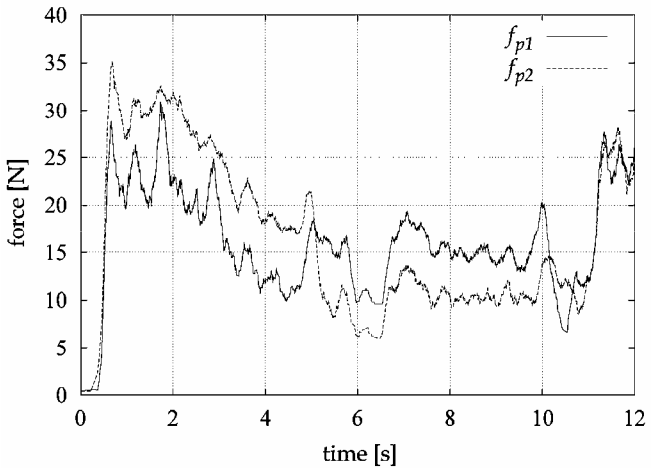

Figure 10 Contact forces of each hand measured from the force sensors during simulation

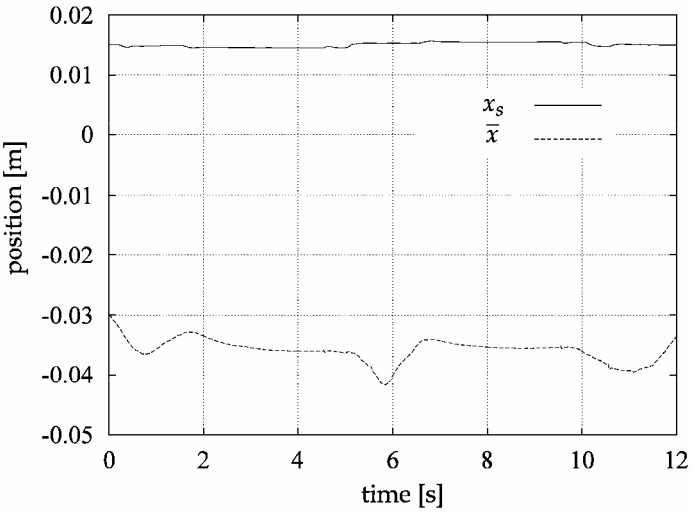

Figure 11. Simulation result of the x component of static balancing point (p_s) and CoM position (p) during the manipulation. The static balancing point is maintained during simulation

Fig. 10 shows the simulation results of the contact forces f_{p1}, f_{p2} for right and left hands respectively. The robot hands are approaching to the object at the dose positions at t=0 [sec]. As shown in the figure, the contact occurs at around f=0.8 [sec]. Then both the contact forces stabilize around the desired force f_{xd}=25[N] by t=1.0 [sec]. The manipulation starts at this moment and lasts for 10[sec] as indicated in Table 1. We can observe that the contact force decreased during the manipulation. It may be because the arms go to a stretched

configuration where it is difficult to generate the force in the desired direction during manipulation especially for the position controlled arm. However, the forces regain the desired value after the manipulation is finished at t=11 [sec]. From this simulation result of measured contact force, it is verified that the usage of impedance control for contact force is sufficiently effective.

The x coordinates of static balancing point $\boldsymbol{p}_s$ and CoM position $\overline{\boldsymbol{p}}$ without external force, x_s and $\overline{x}$, plotted in Fig. 11. Here $\overline{\boldsymbol{p}}$ represents an approximated movement of the waist position. Without balance controlling, x_s would keep increasing as the robot reaches out the arms and force is applied to the hand during the manipulation until the robot falls down. In the graph, the static balancing point is regulated by moving the waist position so that it coincides with the center of the feet (shift along x-axis of 0.015[m]) according to the balancing control.

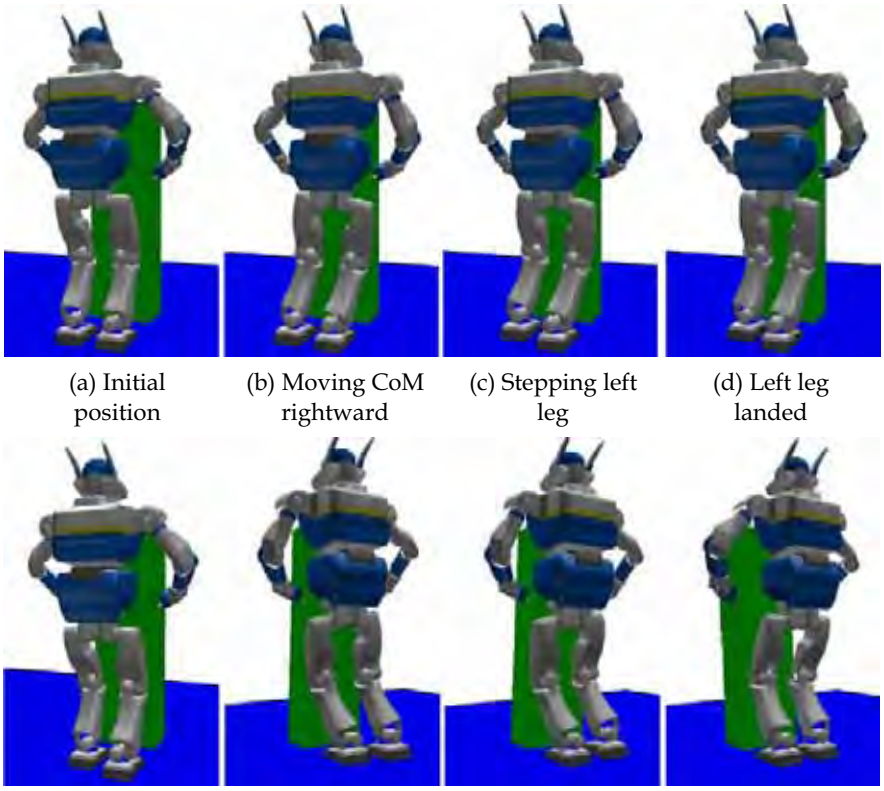

(a) Initial position (b) Moving CoM rightward (c) Stepping left leg (d) Left leg landed

(e) Moving CoM center (f) Moving CoM leftward (g) Stepping right leg (h) Stepping finished

Figure 12. Stepping forward keeping the hands on the object using RMC. First making a step by supporting on left foot (a) - (d), then another step on right leg (e) - (h) by keeping the CoM inside the support polygon

The robot motion phase is simulated based on the proposed method. Fig. 12 shows the sequence of stepping for forward motion. After the manipulation, the robot steps forward

by 50[mm] by moving its feet alternatively with the hands fixed on the object, using RMC to maintain the whole body balance. As shown in Fig. 12, first robot moves its CoM on the right foot and then moves the left foot forward. The same sequence is repeated for the right foot. The simulation shows that robot can effectively moves towards the desired direction of manipulation.

6. Experimental Results

We have conducted an experiment of the manipulation control part in the same condition as in simulation using HRP-2 humanoid hardware platform. Thanks to the architecture of OpenHRP with binary compatibility with the robot hardware, the developed simulation software can be directly utilized in hardware without modification.
Fig. 13 shows snapshots of the experiments using a box of the same size and weight as in simulation. As can be seen, the pivoting manipulation has been executed appropriately and the displacement in x direction was around 0.06[m] as expected from simulation.

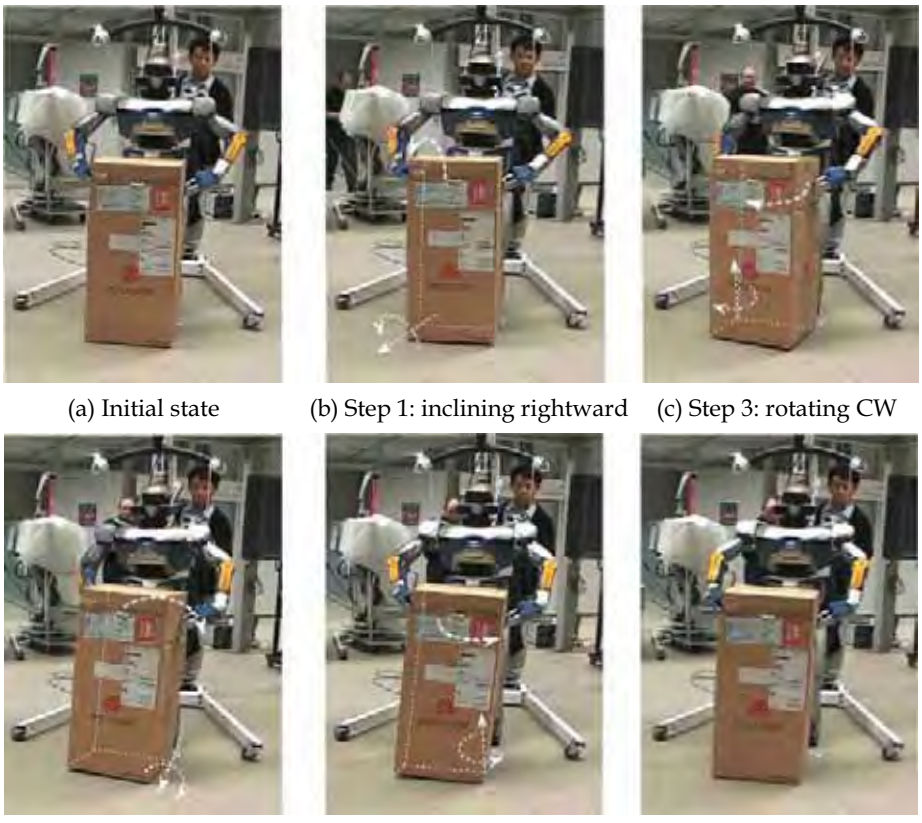

(a) Initial state (b) Step 1: inclining rightward (c) Step 3: rotating CW

(d) Step 4: inclining leftward (e) Step 5: rotating CCW (f) Final state

Figure 13. Experiment of pivoting motion. Starting from the initial position (a), first the object is inclined (b) to rotate clockwise horizontally (c). Then the humanoid robot inclines the object on the other vertex (d) to rotate counter-clockwise (e) to finish the manipulation (f)

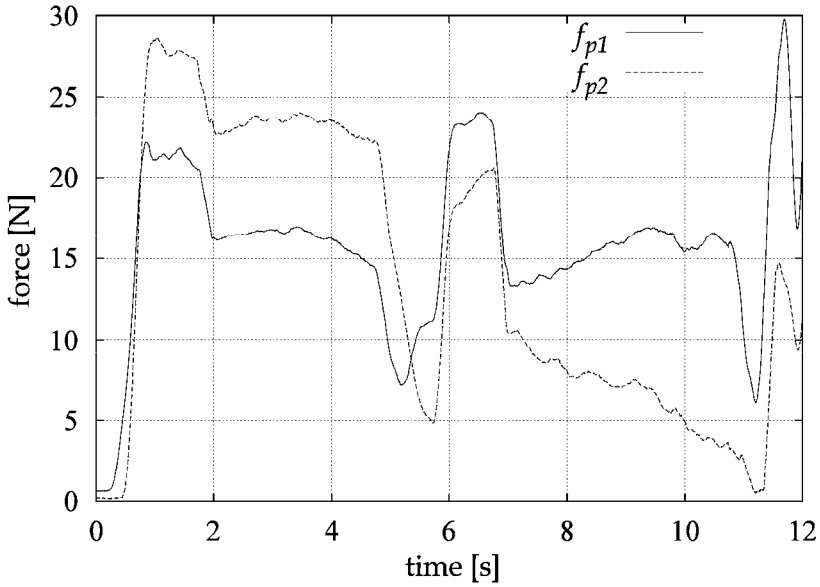

Figure 14. Experimental result of contact forces of each hand. The grasping start at t=1[sec] and finish in 10 seconds. Enough force for the manipulation is maintained but

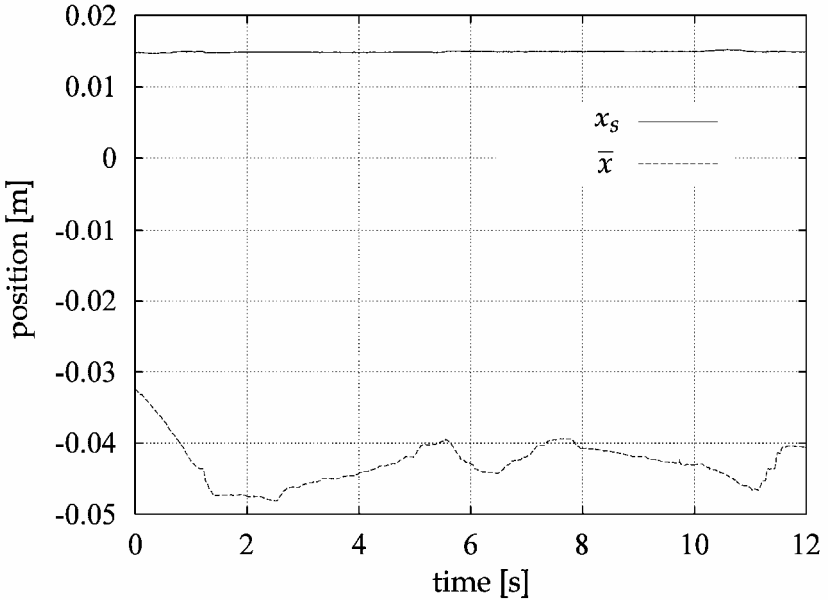

Figure 15. Experimental result of static balancing point (x_s) and CoM position !!!(x). The static balancing point is maintained near the center of the support polygon (x=0) by changing the waist position

The experimental result of contact forces measured from wrist force sensors is shown in Fig. 14. Although the measured force shows similar characteristics with the simulation, one of the forces drops drastically from desired force of 25 [N] at the end of manipulation even though it was enough to execute the manipulation task. This is considered to come from the stretched configuration of arm that makes it difficult to generate desired force to hold the object. The manipulation experiment was successful; however, the control of arm configuration and grasping position need to be investigated for more reliable manipulation. The experimental result of the static balancing point and CoM position plotted in Fig. 15 shows the effectiveness of balance control to keep the static balancing point in stable position during the manipulation.
To conclude the experimental results, we could verify the validity of proposed pivoting manipulation based on whole-body motion.

7. Conclusions

In this paper a pivoting manipulation method has been presented to realize dexterous manipulation that enables precise displacement of heavy or bulky objects. Through this application, we believe that the application area of humanoid robot can be significantly extended.
A sequence of pivoting motion composed of two phases has been proposed, manipulation control and robot stepping motion. In the former phase, an impedance control and balancing control framework was introduced to control the required contact force for grasping and to maintain stability during manipulation respectively. Resolved momentum control is adopted for stepping motion in the latter phase.
We then showed a sequence of pivoting motion to transport the objects towards the desired direction. We have shown that the proposed pivoting manipulation can be effectively performed by computer simulation and experiments using a humanoid robot platform HRP-2.
As a future work, the method will be improved to adapt to various object shapes of transportation in pursuit of wide application in future developments. One of other extension is the manipulation planning for more general trajectories with experimentation of both manipulation and stepping phases. Integration of identification of physical properties of the objects or environments (Yu et al., 1999, Debus et al., 2000) is also an important issue to improve the robot's dexterity.

8. References

Y. Aiyama, M. Inaba, and H. Inoue (1993). Pivoting: A new method of graspless manipulation of object by robot fingers, *Proc. of the IEEE/RSJ Int. Conf. on Intelligent Robots and Systems*, 136 -143,1993.

S. Kajita, F. Kanehiro, K. Kaneko, K. Fujiwara, K. Harada, K. Yokoi, and H. Hirukawa (2003). Resolved momentum control: Humanoid motion planning based on the linear and angular momentum, *Proc. of IEEE/RSJ Int. Conf. on Intelligent Robots and Systems*, 1644-1650, 2003.

M. Mason (1986). Mechanics and Planning of Manipulator Pushing Operation, *Int. J. Robotics Research*, 5-3,53-71,1986.

K. Lynch (1992). The Mechanics of Fine Manipulation by Pushing, *Proc. IEEE Int. Conf. on Robotics and Automation*, 2269-2276,1992.

A. Bicchi, Y. Chitour, and A. Marigo (2004). Reachability and steering of rolling polyhedra: a case study in discrete nonholonomy, *IEEE Trans, on Automatic Control*, 49-5, 710-726,2004.

Y. Maeda and T. Arai (2003). Automatic Determination of Finger Control Modes for *Graspless Manipulation, Proc. of IEEE/RSJ Int. Conf. on Intelligent Robots and Systems,* 2660-2665,2003.

H. Yoshida, K. Inoue, T. Arai, and Y. Mae (2002). Mobile manipulation of humanoid robots-optimal posture for generating large force based on statics, *Proc. of IEEE Int. Conf. on Robotics and Automation*, 2271 -2276,2002.

Y. Hwang, A. Konno and M. Uchiyama (2003). Whole body cooperative tasks and static stability evaluations for a humanoid robot, *Proc. of IEEE/RSJ Int. Conf. on Intelligent Robots and Systems*, 1901 -1906,2003.

K. Harada, S. Kajita, F. Kanehiro, K. Fujiwara, K. Kaneko, K. Yokoi, and H. Hirukawa (2004). Real-Time Planning of Humanoid Robot's Gait for Force Controlled Manipulation, *Proc. of IEEE Int. Conf. on Robotics and Automation*, 616-622,2004.

T. Takubo, K. Inoue, K. Sakata, Y. Mae, and T. Arai. Mobile Manipulation of Humanoid Robots Control Method for CoM Position with External Force -, *Proc. of IEEE/RSJ Int. Conf. on Intelligent Robots and Systems,* 1180-1185,2004.

K. Harada, S. Kajita, H. Saito, M. Morisawa, F. Kanehiro, K. Fujiwara, K. Kaneko, and H. Hirukawa (2005). A Humanoid robot carrying a heavy object, *Proc. of IEEE Int. Conf. on Robotics and Automation*, 1724-1729,2005.

N. E. Sian, K. Yokoi, S. Kajita, and K. Tanie (2003). Whole Body Teleoperation of a Humanoid Robot Integrating Operator's Intention and Robot's Autonomy – An Experimental Verification -, *Proc. of IEEE/RSJ Int. Conf. on Intelligent Robots and Systems,* 1651-1656,2003.

F. Kanehiro, N. Miyata, S. Kajita, K. Fujiwara, H. Hirukawa, Y. Nakamura, K. Yamane, I. Kohara, Y. Kawamura and Y. Sankai (2001). Virtual humanoid robot platform to develop, *Proc. of IEEE/RSJ Int. Conf. on Intelligent Robots and Systems*, 1093 -1099, 2001.

K. Kaneko, F. Kanehiro, S. Kajita, H. Hirukawa, T. Kawasaki, M. Hirata, K. Akachi and T. Isozumi (2004). The Humanoid Robot HRP-2, *Proc. of IEEE/RSJ Int. Conf. on Robotics and Automation*, 10831090, 2004.

Y. Yu, K. Fukuda, and S. Tsujio (1999). Estimation of Mass and Center of Mass of Graspless and Shape-Unknown Object, *Proc. of IEEE Int. Conf. on Robotics and Automation*, 2893-2898, 1999.

T. Debus, P. Dupont and R. Howe: Automatic Identification of Local Geometric Properties During Teleoperation, *Proc. of IEEE International Conference on Robotics and Automation*, 3428 -3434, 2000.